JCTC Journal of Chemical Theory and Computation

Article

pubs.acs.org/JCTC

Molecular Force Field Development for Aqueous Electrolytes: 1. Incorporating Appropriate Experimental Data and the Inadequacy of Simple Electrolyte Force Fields Based on Lennard-Jones and Point Charge Interactions with Lorentz−Berthelot Rules

Filip Moučka,[†,‡] Ivo Nezbeda,[‡,§] and William R. Smith*[,†]

[†]Faculty of Science, University of Ontario Institute of Technology, Oshawa, ON L1H7K4, Canada

[‡]Faculty of Science, J. E. Purkinje University, 400 96 Ústí n. Lab., Czech Republic

[§]E. Hála Laboratory of Thermodynamics, Institute of Chemical Process Fundamentals, Academy of Sciences, 165 02 Prague 6, Czech Republic

ABSTRACT: It is known that none of the available simple molecular interaction models of aqueous electrolytes based on SPC/E water and their associated force fields are able to reproduce the concentration dependence of important thermodynamic properties of even the simplest electrolyte, NaCl, at ambient conditions over the entire experimentally accessible concentration range [Moučka, F.; Nezbeda, I.; Smith, W. R. *J. Chem. Phys.* **2013**, *138*, 154102]. This paper explores the possibility of improving their performance by incorporating concentration-dependent experimental data for the total ionic chemical potential and the density into the fitting procedure, in addition to experimental values of solubility and solid chemical potential. We describe a general parameter estimation methodology for a studied class of models that incorporates the aforementioned experimental data. When the entire concentration range is considered, although the resulting force field is a slight improvement over others currently available in the literature, overall quantitative agreement with the experimental data over this range remains unsatisfactory. This indicates an inherent limitation of such simple molecular interaction models and strongly suggests that more complex mathematical forms of such models are required to quantitatively predict the properties of aqueous electrolyte solutions when the entire concentration range is of interest. Our parameter estimation methodology is also applicable to such cases.

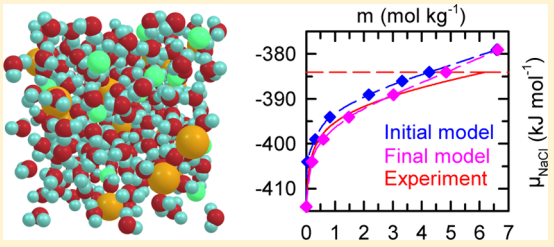

1. INTRODUCTION

Aqueous electrolyte solutions are both of fundamental scientific interest and of importance in applications to biological, geochemical, and industrial systems. Advances in computer technology and classical molecular simulation techniques have enabled the prediction of the macroscopic properties of these and other systems, based on mathematical models of the underlying molecular interactions and their implementation with specified parameter values [the molecular force field (FF)]. The quality of such predictions is dependent on the details of the FF, whose parameters are typically determined by fitting to a specific set of experimental data. It is important that a FF be transferable to thermodynamic conditions and systems other than those used for the determination of its parameters. This includes, for example, its use over a relevant temperature, pressure, and composition range and also in mixtures involving other components.

Two main factors determine the suitability and accuracy of a FF's predictions of system properties: (1) the mathematical form of its molecular interaction model and (2) the experimental data used to determine its parameters. In spite of much previous work, there is no consensus regarding the selection of a satisfactory molecular interaction model for aqueous electrolyte solutions, even for the simplest case of NaCl at ambient conditions. The same conclusion applies to the choice of experimental data, with most previous studies utilizing various types of primarily low concentration data, which cannot be expected to lead to good results at higher concentrations.

For factor (1), FFs for aqueous electrolyte solutions depend on the specific water FF used, and the water−ion portion of the FF and its parameters are thus specific to every particular water FF. The list of available such FFs for water is enormous,[1,2] but only a handful of these have actually been used in conjunction with electrolytes, primarily the SPC,[3] SPC/E,[4] and TIP *i*P-type[2] FFs. The simplest ionic FFs in common use are based on a molecular interaction model of charged Lennard-Jones (LJ) spheres in conjunction with these water FFs.

A crucial role is also played by factor (2), concerning the experimental data chosen for determining the parameters of a given interaction model. A plethora of possibilities exists, and it is important to select properties that are simultaneously important in applications, sufficiently sensitive to the FF

Received: July 10, 2013
Published: October 8, 2013

Table 1. Ion−Ion Interaction Parameters and Calculated Properties of NaCl for the Force Fields of Joung and Cheatham (JC),[9] Horinek et al. (H2),[10] the FF0 and FF1 Force Fields of This Study, and Corresponding Experimental Values

model	$\sigma_{ii}(Na^+)$ (nm)	$\varepsilon_{ii}(Na^+)$ (kJ mol^{-1})	$\sigma_{ii}(Cl^-)$ (nm)	$\varepsilon_{ii}(Cl^-)$ (kJ mol^{-1})	solid chemical potential, μ_c (kJ mol^{-1})	solid density, ρ_s (kg m^{-3})	solubility,[a] m_s^{int} (mol kg^{-1})	solubility,[b] m_s (mol kg^{-1})
JC	0.2160	1.47546	0.4831	0.05349	−384.37	2010.88(4)	3.6(2)	3.7(2)
					−384.12[27]		4.8(3)[27]	4.8(3)[27]
					−389.1[26]		0.85(15)[26]	
							7.27[c34]	
							5.5(4)[c27]	
H2	0.2130	1.54002	0.4400	0.42000	−386.91	1915.02(4)	1.75(15)	2.55(20)
FF0	0.2220	0.94782	0.4547	0.16388	−391.38	2030.82(4)	1.46(15)	4.26(20)
FF1	0.2075	1.32374	0.4579	0.20733	−388.08	1978.61(4)	3.37(20)	4.85(20)
experiment					μ_c^{exp}	ρ_s^{exp}	m_s^{exp}	
					−384.024[37]	2165[39]	6.15[28]	

[a]Obtained from equality of the chemical potentials of the liquid and solid phases using the FF for both phases. [b]Obtained from equality of the chemical potential of the liquid phase FF and the experimental value of the solid chemical potential. [c]Obtained from molecular dynamics simulations using a slab geometry.

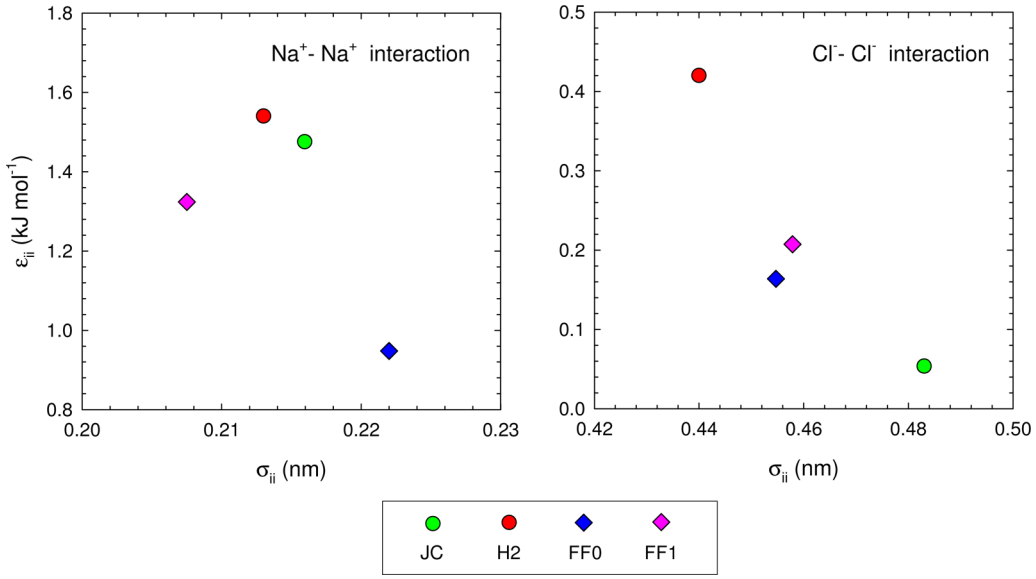

Figure 1. Graphical representation of the σ_{ii} and ε_{ii} values of the indicated force field parameters for the Na^+ (left) and Cl^- (right) ions.

parameters, and can be conveniently calculated in a simulation. The last consideration seems to have played a dominant role in FF development, with the vast majority of studies using properties readily calculated by molecular dynamics packages such as GROMACS,[5] AMBER,[6] and CHARMM.[7] Thus, infinite dilution properties of single ions such as hydration free energy, enthalpy, and entropy have been used,[8−11] in addition to properties related to the water−ion radial distribution function at these conditions.[8] The density dependence at relatively low concentrations[12,13] and solid salt properties, such as lattice constants, have also been used.[9,14] Finally, several research groups have used the Kirkwood-Buff integrals,[15] which relate integrals of the radial distribution functions to experimental values of the compressibility, density, and activity coefficient derivatives[14,16−18] at a given concentration.

The applicability of a FF for aqueous electrolytes over the entire experimentally accessible concentration range is an important criterion for judging its quality. Among the most important such properties are the solution density and the total electrolyte chemical potential. It is necessary to predict the former with reasonable accuracy because a model unable to do this will very likely predict the microscopic structure of the modeled system incorrectly, and consequently, the accuracy of thermodynamic properties determined therefrom will be negatively affected. In addition to its importance in bulk systems, the chemical potential also plays a significant role in molecularly confined systems (e.g., electrolytes in slits or pores): it is an input parameter in open ensemble simulations used for modeling such systems and must thus be determined quite accurately since even a small inaccuracy in the bulk solution chemical potential can potentially give rise to a very large error in the resulting equilibrium concentration in the confined phase.

From the technical point of view, it is worth mentioning that the evaluation of the concentration dependence of the electrolyte chemical potential by means of molecular simulations can be a formidable computational task, and apart from our own studies,[19−23] we are aware of only four other studies in the literature dealing with this dependence up to the solubility limit.[24−27]

With respect to the above facts, we recently examined 13 of the most common FFs in this respect, selected from the above-mentioned studies that are based on SPC/E water and charged

dx.doi.org/10.1021/ct4006008 | J. Chem. Theory Comput. 2013, 9, 5076−5085

Lennard-Jones ionic models[22] and which are widely used in simulation packages. We studied the predictions of these FFs for aqueous NaCl at ambinent conditions with respect to the concentration dependence of the solution density and of the total ionic molar chemical potential, μ, in addition to the electrolyte solubility and the chemical potential and density of the crystalline solid. We found that the majority of these FFs fail to accurately predict the experimental behavior of $\overline{v}(m)$ and of $\mu(m)$, where $\overline{v}$ is the specific volume (the reciprocal of the mass density, which displays differences more readily) and m is the solution molality, with some even exhibiting solid precipitation at concentrations well below the experimental solubility limit, $m_s^{exp} = 6.15$ mol kg^{-1}.[28] FFs developed by fitting experimental hydration free energies give relatively good μ values at low concentrations, whereas others perform less well. None of the FFs performs well for calculating μ at high concentrations. The majority do not even accurately capture the experimental values of the density at moderate concentrations. Finally, the calculated values of the molar solid chemical potentials, μ_c, are spread over a range of values, as are the predicted solubilities. We concluded that the best performing (although not quantitatively accurate) FFs of those studied are the FF of Joung and Cheatham (JC)[9] and a FF due to Horinek et al. (H2).[10] The parameters of these FFs are given in the second and third rows of Table 1, along with their selected predicted results, and a graphical representation of the parameter values is depicted in Figure 1.

This paper is the first of an intended series whose ultimate goal is to develop a new generation of FFs for aqueous electrolytes, capable of being used over the entire concentration range and transferable to other thermodynamic conditions and different molecular environments. This ultimately involves the development of FFs based on interaction models employing the best available choices for water and for the ion−water and ion−ion interactions. Nonetheless, even FFs based on simple interaction models may have the potential to produce improved results by more appropriate choices of experimental data and better methods for determining the parameters in conjunction with such data. In the present study, we thus consider the possibility that FFs based on SPC/E water and charged Lennard-Jones spheres may produce better results than heretofore available, provided more appropriate experimental data are used for estimation of the FF parameters, in conjunction with improved parameter estimation methods for their determination.

In the next section of the paper, we discuss the details of the molecular interaction models and the simulation methodology used. The subsequent section describes our methodology for determining the FF parameters, followed by a section presenting and discussing our results. The final section contains our conclusions and recommendations for future work.

2. MOLECULAR INTERACTION MODELS AND SIMULATION METHODOLOGY

We model water using the standard SPC/E force field.[4] For NaCl, we consider a model for the ion−ion and ion−water interactions for which the interactions between all types of particles are modeled by a sum of Lennard-Jones (LJ) interactions

$$U_{ij,\mathrm{LJ}} = 4\varepsilon_{ij}\left[\left(\frac{\sigma_{ij}}{r_{ij}}\right)^{12} - \left(\frac{\sigma_{ij}}{r_{ij}}\right)^{6}\right] \equiv \frac{c_{12,ij}}{r_{ij}^{12}} - \frac{c_{6,ij}}{r_{ij}^{6}} \quad (1)$$

and Coulombic interactions

$$U_{ij,\mathrm{Coul}} = \frac{q_i q_j}{4\pi\varepsilon_0 r_{ij}} \quad (2)$$

where ε_{ij} and σ_{ij} are, respectively, the LJ well depth and LJ size parameters, r_{ij} is the distance between the interacting sites i and j, q_k is the charge at the center of the interacting site k, and ε_0 is the permittivity of free space. The model embodies a single LJ site that coincides with either the center of the oxygen atom (O) for the water or the ion centers. To comply with common practice and to ensure transferability of all aspects of the FF, we use the Lorentz−Berthelot combining rules for the cross LJ parameters, ε_{ij} and σ_{ij}:

$$\sigma_{ij} = \frac{\sigma_{ii} + \sigma_{jj}}{2} \qquad \varepsilon_{ij} = \sqrt{\varepsilon_{ii}\varepsilon_{jj}} \quad (3)$$

To calculate the system density, we used standard NPT Monte Carlo simulations.[29] For chemical potential computations, we used the Osmotic Ensemble Monte Carlo (OEMC) algorithm, which is described in detail in our previous papers;[19−21] the chemical potential reference states, corresponding to the usual experimental convention, are also described in these papers. An externally imposed chemical potential serves as an input parameter for an OEMC simulation, which calculates the corresponding molality. To calculate the chemical potential of crystalline NaCl, we employed thermodynamic integration using the Einstein crystal approach.[30,31]

All simulations were carried out in a cubic simulation box with periodic boundary conditions. In order to make contact with the results of other workers,[25−27] in the case of liquid systems, we used 270 water particles, and the number of alkali−halide ion pairs in the box varied depending on the studied system and the externally imposed solid chemical potential. The crystals were simulated using 500 ion pairs, and the thermodynamic integration comprised 64 steps gradually changing the interactions of the particles. We used the same value of the cutoff radius for both the LJ and Coulombic interactions, r_c = 9 Å, and we treated the long-ranged Coulombic interactions using the Ewald summation method.[29] (We remark that some of our early calculations employed the Generalized Reaction Field methodology.[32]) Initially, the particles were placed on a face-centered cubic lattice, and rotations of the molecules were generated randomly in the case of liquid systems; the simulations of solids started from the ideal NaCl crystalline lattice, and the initial configurations were then equilibrated. For further details, see our recent OEMC paper.[21]

3. ESTIMATION OF THE FORCE FIELD PARAMETERS

The water−water interactions are defined by the original SPC/E force field, and we herein describe in detail the procedure we used for determining the parameters for the intermolecular interactions of the Na^+ and Cl^- ions in eq 1. Setting the charges q_i of the ions to $\pm e$, where e is the electronic charge, e = 1.602189 × 10^{-19} C, there remain four non-electrostatic LJ

parameters to be determined: σ_{ii} and ε_{ii} for each of the Na^+-Na^+ and Cl^--Cl^- interactions, hereafter denoted by the parameter vector $\mathbf{p} = (\sigma_{Na^+}, \varepsilon_{Na^+}, \sigma_{Cl^-}, \varepsilon_{Cl^-})$. The parameters of the unlike ion−ion or ion−(water oxygen) interactions are obtained from $\mathbf{p}$ using eqs 3.

To obtain the parameters, we used an iterative procedure based on the Newton−Raphson (NR) method, which systematically improves selected properties of the simulated solution, starting from a reasonable initial parameter estimate, $\mathbf{p}^0$. In the following two subsections, we describe our criteria to which the NR method is applied and the determination of $\mathbf{p}^0$.

3.1. Criteria for Estimating the Parameters. As explained in the Introduction, because of their importance for concentrated solutions, we base our criteria on the FF's predictions of the concentration dependence of its total molar ionic electrolyte chemical potential $\mu \equiv \mu(Na^+) + \mu(Cl^-)$, the solubility, the solid chemical potential, and of its specific volume, $\bar{v}$. The criteria are motivated by the following observations.

Our findings from our previous studies[21,22] can be described in the context of Figure 2, which shows the generic behavior of

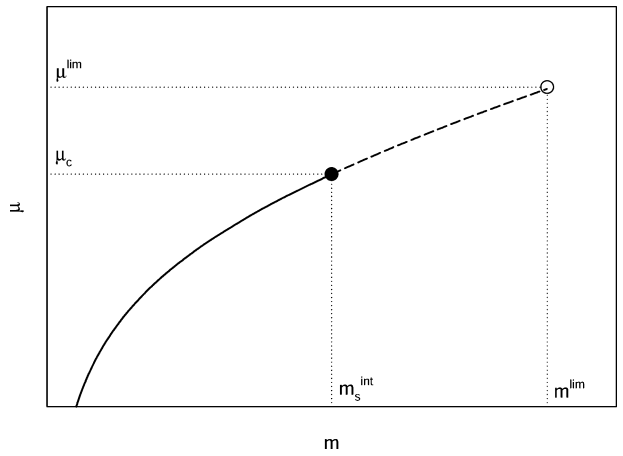

Figure 2. Schematic representation of the dependence of the total molar ionic electrolyte chemical potential on molality, $\mu(m)$, resulting from OEMC simulations for a given FF. The m_s^{int} is the "intrinsic solubility" predicted by the FF when it is used for both solution and crystalline phases; μ_c is the chemical potential of the solid; m^{lim} is the concentration corresponding to the limiting chemical potential μ^{lim}. The dashed portion of the curves represents supersaturated thermodynamically metastable states, corresponding to reproducible OEMC results.

$\mu(m)$ from the OEMC simulations for a typical FF. A key feature is the curve's termination at an upper concentration limit, m^{lim}, corresponding to a limiting chemical potential, μ^{lim}. The "intrinsic solubility", m_s^{int}, is the concentration corresponding to the chemical potential of the crystalline solid with the same FF, μ_c. The dashed portion of the curve, although representing supersaturated thermodynamically metastable states, corresponds to reproducible OEMC results; we remark that supersaturated states are also reproducible experimentally (e.g., ref 33). Chemical potential values greater than μ^{lim} give rise to divergent OEMC simulations, in which the amount of the crystalline solid phase increases without limit. We conclude that this implies that simulations in other ensembles at concentrations greater than m^{lim} are suspect since they would contain both crystalline and solution phases. Although this may be difficult to detect in such simulations, we have observed this by visual inspection in an NPT simulation.[22] Consequently, if the experimental solubility, m_s^{exp} (not shown in the diagram), lies above m^{lim}, the FF is of limited use.

A key additional feature of the $\mu(m)$ curve depends on the location of the experimental crystalline chemical potential, μ_c^{exp} (again, not shown in the diagram), relative to μ^{lim}. The solubility m_s occurs at the point on the curve where μ is equal to μ_c^{exp}. If $\mu_c^{exp} > \mu^{lim}$, m_s cannot be calculated by the OEMC algorithm; we also believe that it cannot be *reliably* calculated using other methods. In summary, an optimal FF with respect to solid chemical potential and solubility predictions will result in $m_s = m_s^{int} = m_s^{exp}$ and $\mu_c = \mu_c^{exp}$.

Values of $\mu(m)$ and the molar solid chemical potential, μ_c, for the JC and H2 FFs are shown in Figure 3. The values of μ_c, m_s,

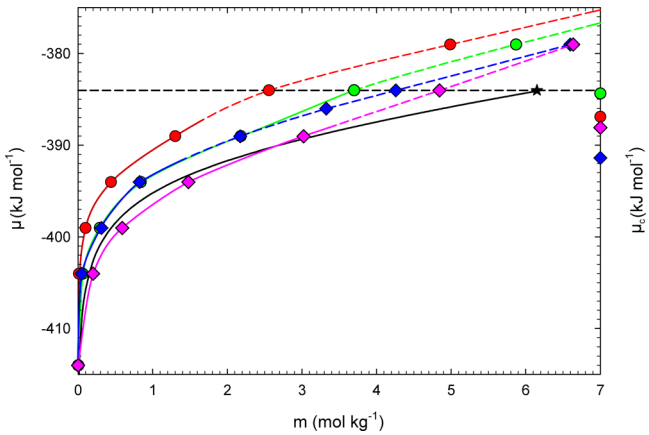

Figure 3. Dependence of the total molar ionic electrolyte chemical potential on molality, $\mu(m)$, for aqueous NaCl at T = 298.15 K and P = 1 bar for the indicated force fields. The experimental results, indicated by the solid black curve, are taken from Hamer;[28] the asterisk denotes the termination of the experimental curve at the solubility limit; the solid portions of the curves denote undersaturated states, and the dashed portions denote supersaturated states. See the legend to Figure 1 for definitions of the other symbols. The symbols on the right axis denote the values of the solid chemical potentials, μ_c, predicted by the corresponding force fields.

and m_s^{int} are given in Table 1. Our value of μ_c for the JC FF agrees with that of Aragones et al.[27] and disagrees with that of Paluch and Maginn.[26] The latter group's result is in error, as pointed out by Aragones et al.[27] The values of m_s^{int}, calculated using different methodologies, mutually disagree. The result of Paluch and Maginn[26] is incorrect, in view of their erroneous calculation of μ_c. Our result and that of Aragones et al.[27] disagree somewhat, and this merits further study. We note, however, that the value of m_s is very sensitive to the details of the simulation methodology, due to the small slope of $\mu(m)$ at higher concentrations. Finally, the results of Joung et al.[34] and of Aragones et al.[27] obtained using MD simulations in a slab geometry disagree. The latter discussed the problematic nature of this methodology with respect to length of simulation runs and finite system size. Furthermore, we remark that special methods must be applied in inhomogeneous systems for long-range corrections due to non-electrostatic interactions,[35] and it is not clear whether these were applied in their simulations for the different FFs.

The $\mu(m)$ curves for the different FFs are mutually shifted, and their shapes are slightly different; however, their course can be reasonably controlled by two conveniently chosen points,

dx.doi.org/10.1021/ct4006008 | J. Chem. Theory Comput. 2013, 9, 5076−5085

for example, by the values of molality at two values of μ, one yielding a molality in a high concentration region and the other resulting in a moderate or low concentration. If necessary, another point could be added to more firmly fix the shape of the curve.

The experimental results for the concentration dependence of $\overline{v}$ and the predictions of the best available existing FFs (JC and H2) are shown as circles and their associated curves in Figure 4 for $m \geq 0.2$. At lower concentrations (not shown), all

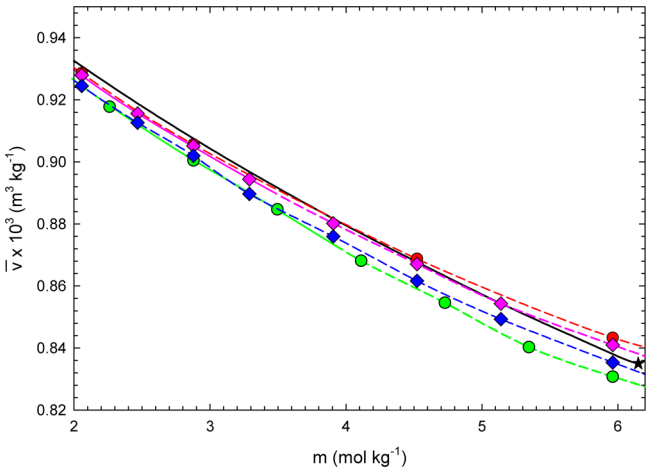

Figure 4. Dependence of the specific volume on molality, $\overline{v}(m)$, for aqueous NaCl at T = 298.15 K and P = 1 bar at moderate and high concentrations for the indicated force fields. The statistical uncertainties of the results lie within the size of the symbols. The experimental results, indicated by the solid black curve, are taken from Rogers and Pitzer.[36] The solid portions of the curves denote undersaturated states below the solubility calculated from equality of the solution and solid chemical potentials when both quantities are calculated using the same the FF (the "intrinsic solubility" of the FF described in the text). See the legend to Figure 1 for definitions of the other symbols.

curves smoothly extrapolate to the specific volume of SPC/E water, $\overline{v}(0)$. The $\overline{v}(m)$ curve is not complicated. Since $\overline{v}(0)$ is independent of the ionic FF, the entire curve is well determined by a single point at a reasonably high molality.

On the basis of the above observations, we determined the parameter vector $\mathbf{p}$ for NaCl by attempting to match its predictions with the following four experimental quantities in eqs 4−7, indicated by the superscript (exp):

$$\rho_h(m_h^{exp}; \mathbf{p}) = \rho_h^{exp}(m_h^{exp}) \quad (4)$$

where ρ_h is the simulated density at the concentration m_h^{exp} = 4.523 mol kg^{-1}, corresponding to a system of 22 ion pairs in 270 water molecules. This value of molality was chosen as being representative of the relatively high concentration region. The corresponding experimental value of the density is ρ_h^{exp} (m_h^{exp}) = 1152.34 kg m^{-3}.[36]

$$m_s(\mu_c^{exp}; \mathbf{p}) = m_s^{exp} \quad (5)$$

where m_s^{exp} is the experimental solubility and m_s is the simulated concentration resulting from setting the total electrolyte chemical potential to μ_c^{exp}, that is, $m_s(\mu_c^{exp};\mathbf{p})$ is the solubility predicted by the FF using the experimental value of the solid chemical potential, μ_c^{exp}; μ_c^{exp} = −384.024 kJ mol^{-1}[37] and m_c^{exp} = 6.15 mol kg^{-1}.[28]

$$m_l(\mu_l^{exp}; \mathbf{p}) = m_l^{exp}(\mu_l^{exp}) \quad (6)$$

where m_l is the simulated concentration resulting from setting the total electrolyte chemical potential, μ_l^{exp}, to −394.024 kJ mol^{-1} (a value somewhat below the experimental value of the solid chemical potential), and $m_l^{exp}(\mu_l^{exp})$ is the experimental value at this chemical potential. The choice of μ_l^{exp} is based on the observation that it yields a relatively low concentration value, which fixes the shape of the chemical potential versus concentration curve in this region; $m_l^{exp}(\mu_l^{exp})$ = 1.29 mol kg^{-1}.[28]

$$\mu_c(\mathbf{p}) = \mu_c^{exp} \quad (7)$$

where μ_c is the molar solid chemical potential predicted by the FF. As our intention is to develop high-quality FFs only for solutions and not for solids, this property needs not reproduce the experimental value exactly, but undesirable precipitation occurring below the experimental solubility limit must be avoided, which can be achieved by keeping $\mu_c(\mathbf{p}) \gtrsim \mu_c^{exp}$.

We attempted to satisfy eqs 4−7 by iteratively using the NR method, starting from an initial parameter estimate, $\mathbf{p}^0$, and performing a line search along the direction of the NR parameter−change vector. This procedure was terminated when the equations were satisfactorily solved or further progress was deemed to be impossible. The latter result indicates that either no solution to the equations exists or that the iterations have not converged.

3.2. Initial Parameter Estimate. Joung and Cheatham (JC)[9] developed their FF in part using the experimental values for the single-ion hydration free energies at infinite dilution of Schmid et al.,[38] which reproduce the known experimental value of the total ion hydration free energy at infinite dilution. As noted by Joung and Cheatham, lack of precise knowledge of the proton hydration free energy can cause differences between the single-ion hydration free energies of different authors. Our previous results[22] showed that the JC FF produces results that are not unreasonable although not quantitatively accurate. We thus incorporate the Schmid et al. data in our initial parameter estimate.

Values of the single-ion hydration free energies, μ_{hyd}, define curves in the variables (σ_{ii},ε_{ii}) for each ion, and these curves were determined by means of molecular simulations by Joung and Cheatham.[9] The results are available analytically in the Supporting Information of their publication, via equations of the form

$$\mu_{hyd}(\sigma_{Na^+}, \varepsilon_{Na^+}) = \mu_{hyd}^{exp}(Na^+) \quad (8)$$

$$\mu_{hyd}(\sigma_{Cl^-}, \varepsilon_{Cl^-}) = \mu_{hyd}^{exp}(Cl^-) \quad (9)$$

where an asterisk denotes the experimental Schmid et al. values.

To fix all four parameters of the initial estimate, two more equations are necessary. For this purpose, we set the strength of the ion−ion attractive dispersion forces for each ion via the value of the quantity c_6, defined by (cf. eq 1):

$$c_{6,ii} = 4\varepsilon_{ii}\sigma_{ii}^6 \quad (10)$$

The values of c_6 for Na^+ and Cl^- can be estimated using Slater−Kirkwood formula and the experimental ionic polarizabilities.[11] We set for our initial estimate

$$4(\varepsilon_{Na^+})(\sigma_{Na^+}^6) = 0.45 \text{ J mol}^{-1} \text{ nm}^6 \quad (11)$$

dx.doi.org/10.1021/ct4006008 | J. Chem. Theory Comput. 2013, 9, 5076−5085

$$4(\varepsilon_{Cl^-})(\sigma^6_{Cl^-}) = 5.8\ \text{J mol}^{-1}\ \text{nm}^6 \quad (12)$$

Equations 8, 9, 11, and 12 determine the initial parameter estimate $\mathbf{p}^0$. We substituted eq 11 into 8 and eq 12 into 9 and solved the resulting equations using simulated annealing to minimize the squares of the residuals. Hereafter, we call this the $\sigma\varepsilon$-solver method for obtaining σ_{ii} and ε_{ii} values from values of c_6 and specified single-ion hydration free energy values. The parameters of the initial FF, which we denote as FF0, are given in the fourth row of Table 1 and are shown as blue diamonds in Figure 1.

4. RESULTS AND DISCUSSION

Following the strategy explained in the preceding section, to assess the quality of FF0, we computed its specific volume, $\overline{v}$, and its molar electrolyte chemical potential, μ, as functions of concentration.

In Figure 4, the blue diamonds and associated curves show the computed $\overline{v}(m)$ curves in comparison with the corresponding experimental results and with those of the JC and H2 FFs. FF0 gives results that lie slightly below the experimental curve. This is a good outcome, but it should be borne in mind that the density of the liquid must be predicted very accurately to produce an accurate pressure in simulations performed at constant volume since even a small inaccuracy in density may produce a very large error in the pressure.

Values of $\mu(m)$ and μ_c for FF0 are shown in Figure 3, and the value of μ_c is given in Table 1. The JC curve for $\mu(m)$ is seen to give better agreement with experiment than does H2. The FF0 chemical potential results lie above the experimental curve and are very similar to the corresponding results of the JC FF at low to moderate concentrations, $m < 2$, and FF0 outperforms the JC FF at higher concentrations. This property is thus reasonably well predicted by FF0. The μ_c is quite low in comparison with the corresponding experimental value, but not so low as to cause spurious premature precipitation at any concentration; this is another encouraging feature of the initial FF.

To summarize, the overall performance of FF0 constructed as described above is comparable to that of the best available FFs in the current literature. However, it does not predict the indicated experimental properties quantitatively.

4.1. Improving the Initial Force Field. To systematically improve the initial FF, we introduce four parameters, Δ_i, which measure deviations from its initial parameter values, defined as follows:

1. Δ_1 represents the deviation of $c_{6,ii}$ for Na^+ from the FF0 value.
2. Δ_2 represents the deviation of $c_{6,ii}$ for Cl^- from the FF0 value.
3. Δ_3 changes the individual free energies of hydration of both ions from the FF0 values while preserving the total ion hydration free energy at infinite dilution. Specifically, Δ_3 is added to the value used for the experimental hydration energy of Cl^- and subtracted from the corresponding value for Na^+.
4. Δ_4 changes the individual free energies of hydration of both ions from the FF0 values by the same amount, thus also changing $\mu(m)$ values at low concentrations.

We conducted an initial sensitivity analysis for the dependence of (ρ_h, m_s, m_l, μ_c) on the model parameters comprising $\mathbf{p}^0$ using several values for each Δ_i, both negative and positive, determining the relevant σ_{ii} and ε_{ii} parameters using the $\sigma\varepsilon$-solver. We plotted graphs visualizing the dependence of each property on each Δ_i and calculated the 16 partial derivatives for use in the NR method at the points where all Δ_i parameters are zero by numerically fitting and then differentiating analytical approximations to the curves. We do not display all 16 graphs here, but we show a typical result. In Figure 5, we show the

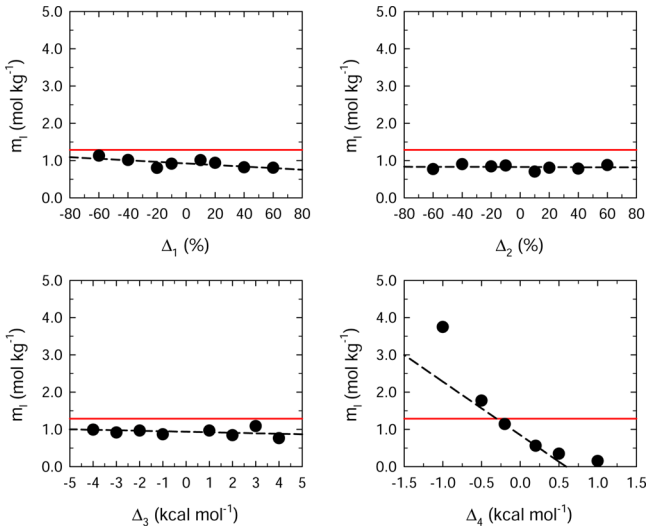

Figure 5. Dependence of m_l, the molality at the relatively low total electrolyte chemical potential, $\mu_l^{exp} = -394.024$ kJ mol^{-1}, as a function of the quantities Δ_i defined in section 4.1 in the neighborhood of the initial estimated force field, FF0. The red horizontal line is the experimental value at this chemical potential (m_l^{exp}), and the dashed lines through the points are regression lines used to calculate the derivatives at $\Delta_i = 0$.

dependence of m_l on the four Δ_i values. It is seen that m_l is strongly dependent on Δ_4 and is relatively independent of the other three parameters within the statistical uncertainties of our simulations. This means that the low concentration region of the $\mu(m)$ curve can only be changed by causing the FF's total hydration free energy to deviate from that obtained from the experimental value of Schmid et al. The experimental value of m_l is reproduced by the FF when $\Delta_4 \approx -0.3$ kcal mol^{-1}, indicating a total hydration free energy at infinite dilution of the FF that is 0.6 kcal mol^{-1} lower than that of Schmid et al. and the corresponding experimental result for this quantity.

We employed the NR method to systematically refine the parameter values. On each iteration, the 16 required partial derivatives were numerically calculated, and we solved the resulting linear equations for the changes in the (Δ_1,Δ_2,Δ_3,Δ_4) parameters. We then performed a line search in the NR direction using a step-size parameter $\lambda \in (0,1]$. We used an increment of 0.1 in λ and calculated the four properties of the corresponding FFs at each λ value; we obtained the parameters in $\mathbf{p}$ using the $\sigma\varepsilon$-solver method. On the basis of the consideration that the predicted properties of the FF should collectively improve (as indicated by the sum of squares of the equation residuals of eqs 4−7) and that μ_c should not be so low as to cause undesirable precipitation, we selected a suitable optimal value of λ to yield the next parameter estimate. We repeated this process until further progress was not possible.

We show the course of our procedure in Figure 6. It is seen that the parameters for Na^+ did not change dramatically on the first NR iteration. The Cl^- parameters moved to much higher σ

dx.doi.org/10.1021/ct4006008 | J. Chem. Theory Comput. 2013, 9, 5076−5085

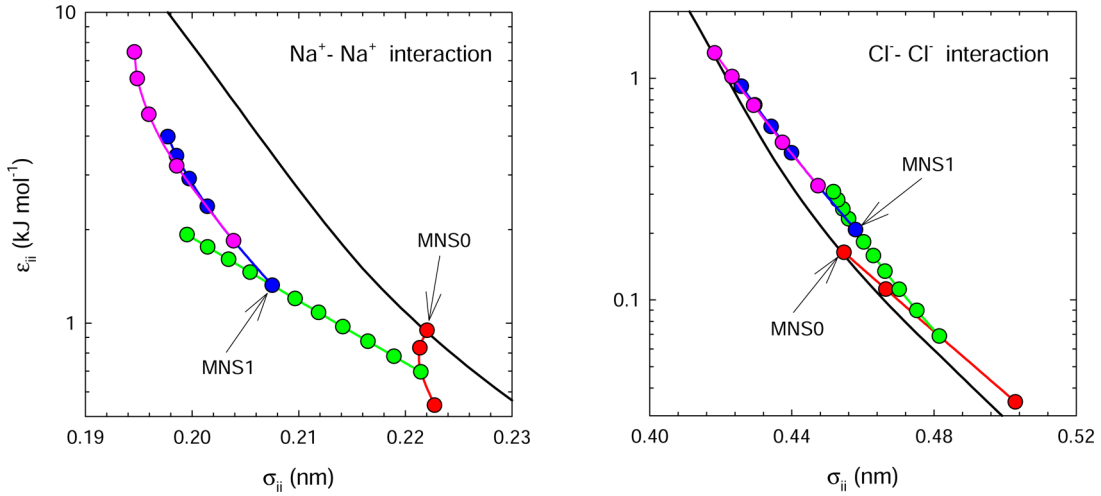

Figure 6. Graphical representation of the course of the σ_{ii} and ε_{ii} values for the Na^+ (left) and Cl^- (right) ions obtained during the iterative procedure improving the initial force field, FF0. The black curves are the results of eqs 8 and 9 of the text.

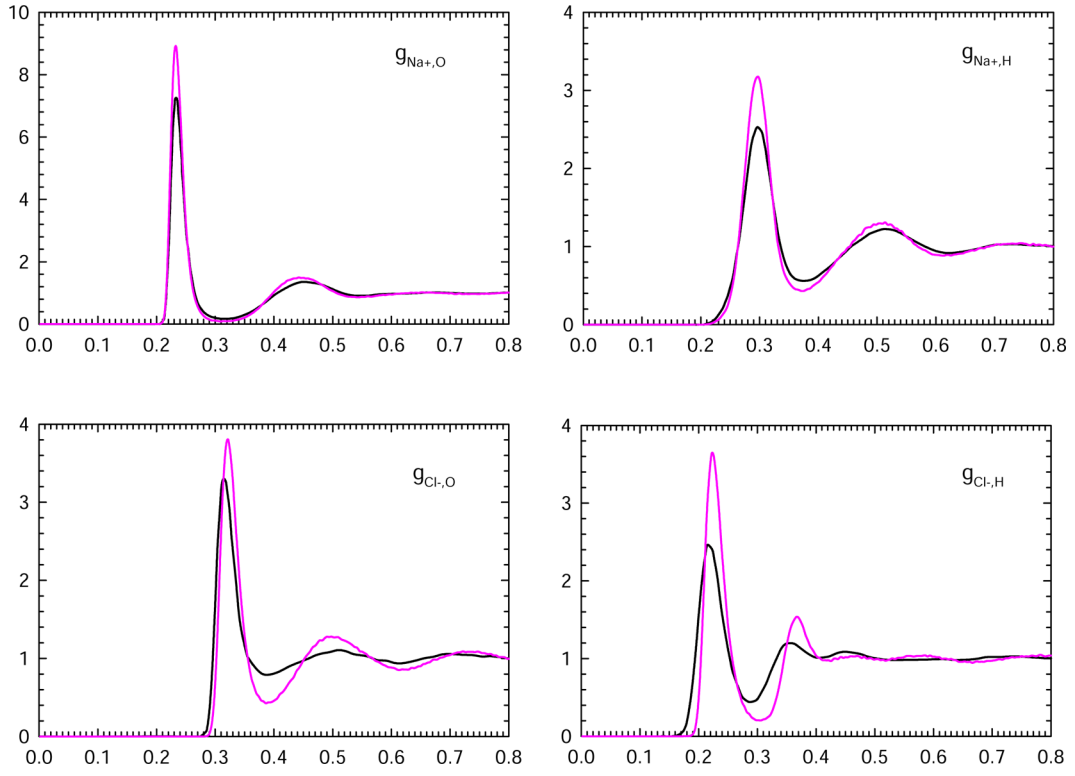

Figure 7. Radial distribution functions for T = 298.15 K, P = 1 bar, and m = 0.6688 mol kg^{-1}, obtained using FF1 (pink) compared to experimental curves[40] (black). Values on the x axis are given in nm.

values and to lower ε values during the first NR iteration, but they returned back to a point rather close to those of the initial FF after the second iteration. We discovered that ρ_h, m_s, and m_l did not change at all along the third line search, but the system precipitated at $\lambda > 0.4$ where μ_c decreased significantly, although its slope, $\partial\mu_c/\partial\lambda$, was close to 0 at $\lambda = 0$. Premature precipitation occurred for $\mu_c \approx -394$ kJ mol^{-1}. Although it seemed that further improvement was impossible, we chose λ = 0.1, where $\mu_c = -388.2$ kJ mol^{-1} was still high enough to avoid precipitation, and we performed another iteration step. The result was not surprising; the new partial derivatives were almost identical with those of the previous step, and consequently, the fourth line search was along almost the same course as the third.

The NR iterations thus did not converge to a set of parameters that satisfied all four criteria. Assuming that the sequence of iterations has not become "trapped" in a local minimum of the sum of squares of the residuals, this indicates that the equations do not have a solution. Notwithstanding, the result obtained after the line search in the second iteration exhibits relatively fairly good behavior when compared with all the other FFs and is the final result of our calculations; we call it FF1.

4.2. Final Force Field. The parameters of the final FF, FF1, obtained by the above-described method are given in Table 1

dx.doi.org/10.1021/ct4006008 | J. Chem. Theory Comput. 2013, 9, 5076−5085

and displayed by the pink diamonds in Figure 1. The value of σ_{ii} for Na^+ decreased by 6.5%, and the ε_{ii} value increased by 40%, resulting in a relatively small decrease of 6.9% in the c_6 value. For Cl^-, σ_{ii} increased slightly (0.7%) and ε_{ii} increased by over 26%, resulting in a relative large increase of 32% in the corresponding c_6 value.

Figure 4 shows the FF1 specific volume curve, $\overline{v}(m)$, where it is compared with experiment and with the results of FF0 and the results of the JC and H2 FFs. We see that FF1 significantly improves this quantity in comparison to FF0. The values of $\overline{v}$ are very close to the experimental curve over the entire range of concentrations. The greatest deficiency is observed at $m \approx 1.6$ mol kg^{-1} (not shown); however, this is still below 3×10^{-6} m^3 kg^{-1}. For high concentrations, $m > 4$ mol kg^{-1}, FF1 performs better than all the other available FFs.

Figure 3 shows the FF1 total molar electrolyte chemical potential curve, $\mu(m)$, as obtained by OEMC simulations using FF1, where it is compared with experiment and with the results of FF0 and the results of the JC and H2 FFs. It is seen that the entire curve is situated lower than that of FF0. In comparison with experiment, FF1 predicts lower μ values at $m \lesssim 3$ mol kg^{-1} and higher values at higher concentrations. At moderate concentrations, $m \approx 3$, it predicts the experimental electrolyte chemical potential almost perfectly. FF1 performs better than all other available FFs for $m \gtrsim 1$ mol kg^{-1}.

The molar solid chemical potential, μ_s, is shown in Figure 3 for FF1, and its value is given in Table 1. The value is about 4 kJ mol^{-1} lower than the experimental value; however, FF1 did not exhibit precipitation, even up to $\mu = -379.024$ kJ mol^{-1}, corresponding to $m = 6.65$ mol kg^{-1}. This means that it can be used for simulating the solution over the entire range of concentrations up to the experimental solubility, $m = 6.15$ mol kg^{-1}, without any undesirable precipitation. FF1 is not suitable for modeling the crystalline phase; for example, its predicted crystalline density is 1978.61 kg m^{-3}, whereas the experimental value is 2165 kg m^{-3}.[39]

Although our approach is aimed at the thermodynamic properties, it is important that the structural properties are also in reasonable concordance with the experimental structure when this is known. We thus calculated all water−water, ion−water, and ion−ion site−site radial distribution functions (RDFs) over the whole range of concentrations at ambient conditions. We show a typical result for these functions in Figure 7, where they are compared with corresponding results obtained from neutron diffraction experiments and empirical potential structure refinement methods (EPSR).[40] It is seen that FF1 reproduces the experimental structure reasonably well. There are some differences between the experimental and predicted RDFs; however, these are typically smaller or comparable to similar results obtained by other state-of-the-art FFs[41] (not shown in the figure). We do not compare our ion−ion RDFs to those obtained by EPSR because neutron diffraction experiments provide no direct information on these without additional assumptions.[40]

Summarizing the features of FF1, (i) it performs better than the best previously available FFs, H2 and JC, at $m \gtrsim 1$ mol kg^{-1}, and (ii) it does not spuriously precipitate. Its greatest deficiency is its total electrolyte chemical potential values at low concentrations, $m \lesssim 1.5$ mol kg^{-1}. Knowledge of the dependence of the properties on the Δ_i parameters allows us to easily correct this deficiency by changing the value of the Δ_4 parameter; however, this would unavoidably shift the entire $\mu(m)$ curve upward toward higher values, harming its usability at higher concentrations.

Finally, we note that the largest differences between the $\mu(m)$ results for FF1 and the corresponding experimental values are less than 6 kJ mol^{-1}. Although this has a large impact on its solubility predictions and, in general, on concentrations obtained by simulations in the open ensemble, it is quite comparable with the inaccuracy of the chemical potential of pure water obtained from the SPC/E FF. The difference between the SPC/E simulation result and the experimental value of the pure water molar chemical potential is about 2 kJ mol^{-1} when the water molecular polarization energy, 5.23 kJ mol^{-1}, is considered, and about −3 kJ mol^{-1} when the polarization energy is not considered.[31,42]

5. CONCLUSIONS

We attempted to develop a new set of parameters for a FF model based on LJ and point charge interactions accompanied by Lorentz−Berthelot rules for aqueous NaCl solutions at ambient conditions that would simultaneously fit the dependence of the chemical potential and density on concentration over the entire experimentally accessible concentration range. However, we were not able to find such a parameter set. We believe that this is not a feature of our fitting algorithm, but rather is a feature of the employed mathematical form of the FF model. Therefore, we do not recommend using this FF model for development of more accurate FFs for NaCl and other alkali−halides. We believe that more complex FF models must be used when the concentration dependence of multiple properties are of interest.

Our parameter fitting algorithm can be easily extended to cases of more complex interaction models involving additional parameters and additional fitted properties (e.g., standard state total electrolyte chemical potential, transport properties, crystal density, etc.). There are many possible ways to increase the complexity of the mathematical form of the FF model from that considered in this paper, including deviating from the Lorentz−Berthelot rules, considering hydrogen−anion repulsion, employing an exponential repulsion term instead of the r^{-12} term in eq 1, spatially distributing charges instead of using point charge sites, and incorporating molecular polarizability. It is not clear which of these routes is best able to positively influence the behavior of the FF. Nevertheless, the methodology provided in this paper can be systematically extended to all such cases.

AUTHOR INFORMATION

Corresponding Author

*E-mail: william.smith@uoit.ca.

Notes

The authors declare no competing financial interest.

ACKNOWLEDGMENTS

Support for this work was provided by the Natural Sciences and Engineering Research Council of Canada (Discovery Grant OGP1041), the Ontario Research Fund, Atomic Energy of Canada Limited, the SHARCNET (Shared Hierarchical Academic Research Computing Network) HPC consortium (http://www.sharcnet.ca), the Czech National Science Foundation (Grant No. P208/12/0105), and the Czech Ministry of Education, Youth and Sport (Project No. LH 12019).

REFERENCES

(1) Guillot, B. A Reappraisal of What We Have Learnt during Three Decades of Computer Simulations on Water. *J. Mol. Liq.* **2002**, *101*, 219−260.

(2) Vega, C.; Abascal, J. L. F. Simulating Water with Rigid Non-polarizable Models: A General Perspective. *Phys. Chem. Chem. Phys.* **2011**, *13*, 19663−19688.

(3) Berendsen, H. J. C.; Postma, J. P. M.; van Gunsteren, W. F.; Hermans, J. Interaction Models for Water in Relation to Protein Hydration. In *Intermolecular Forces*; Pullman, B., Ed.; Reidel: Dordrecht, The Netherlands, 1981; pp 341−342.

(4) Berendsen, H. J. C.; Grigera, J. R.; Straatsma, T. P. The Missing Term in Effective Pair Potentials. *J. Phys. Chem.* **1987**, *91*, 6269−6271.

(5) van Gunstern, W. F.; Billeter, S. R.; Eising, A. A.; Hünenberger, P. H.; Krüger, P.; Mark, A. E.; Scott, W. R. P.; Tironi, I. G. *Biomolecular Simulation: The GROMACS Manual and User Guide*; vdf Hochschulverlang: Zürich, 1996.

(6) Case, D. A.; Darden, T. A.; Cheatham, T. E., III; Simmerling, C. L.; Wang, J.; Duke, R. E.; Luo, R.; Walker, R. C.; Zhang, W.; Merz, K. M.; Roberts, B.; Hayik, S.; Roitberg, A.; Seabra, G.; Swails, J.; Goetz, A. W.; Kolossvry, I.; Wong, K. F.; Paesani, F.; Vanicek, J.; Wolf, R. M.; Liu, J.; Wu, X.; Brozell, S. R.; Steinbrecher, T.; Gohlke, H.; Cai, Q.; Ye, X.; Wang, J.; Hsieh, M.-J.; Cui, G.; Roe, D. R.; Mathews, D. H.; Seetin, M. G.; Salomon-Ferrer, R.; Sagui, C.; Babin, V.; Luchko, T.; Gusarov, S.; Kovalenko, A.; Kollman,P. A. *AMBER 12*; University of California: San Francisco, CA, 2012.

(7) Brooks, B. R.; Brooks, C. L., III; Mackerell, A. D.; Nilsson, L.; Petrella, R. J.; Roux, W.; Archontis, G.; Bartels, C.; Boresch, S.; Caflisch, A.; Caves, L.; Cui, Q.; Dinner, A. R.; Feig, M.; Fischer, S.; Gao, J.; Hodoscek, M.; Im, W.; Kuczera, K.; Lazaridis, T.; Ma, J.; Ovchinnikov, V.; Paci, E.; Pastor, R. W.; Post, C. B.; Pu, J. Z.; Schaefer, M.; Tidor, B.; Venable, R. M.; Woodcock, H. L.; Wu, X.; Yang, W.; York, D. M.; Karplus, M. CHARMM: The Biomolecular Simulation Program. *J. Comput. Chem.* **2009**, *30*, 1545−1615.

(8) Dang, L. X. Mechanism and Thermodynamics of Ion Selectivity in Aqueous Solutions of 18-Crown-6 Ether: A Molecular Dynamics Study. *J. Am. Chem. Soc.* **1995**, *117*, 6954−6960.

(9) Joung, I. K.; Cheatham, T. E., III. Determination of Alkali and Halide Monovalent Ion Parameters for Use in Explicitly Solvated Biomolecular Simulations. *J. Phys. Chem. B* **2008**, *112*, 9020−9041.

(10) Horinek, D.; Mamatkulov, S. I.; Netz, R. R. Rational Design of Ion Force Fields Based on Thermodynamic Solvation Properties. *J. Chem. Phys.* **2009**, *130*, 124507.

(11) Reif, M. M.; Hünenberger, P. H. Computation of Methodology-Independent Single-Ion Solvation Properties from Molecular Simulations. IV. Optimized Lennard-Jones Interaction Parameter Sets for the Alkali and Halide Ions in Water. *J. Chem. Phys.* **2011**, *134*, 144104.

(12) Walter, J.; Deublein, S.; Reiser, S.; Horsch, S.; Vrabec, J.; Hasse, M. In *High Performance Computing in Science and Engineering '11*; Nagel, W. E., Kröner, D. B., Resch, M. M., Eds.; Springer: Berlin, 2012; pp 185−199.

(13) Deublein, S.; Vrabec, J.; Hasse, H. A Set of Molecular Models for Alkali and Halide Ions in Aqueous Solution. *J. Chem. Phys.* **2012**, *136*, 084501.

(14) Weerasinghe, S.; Smith, P. E. A Kirkwood−Buff Derived Force Field for Sodium Chloride in Water. *J. Chem. Phys.* **2003**, *119*, 11342.

(15) Kirkwood, J. G.; Buff, F. P. The Statistical Mechanical Theory of Solutions. I. *J. Chem. Phys.* **1951**, *19*, 774−777.

(16) Smith, P. E. The Effect of Urea on the Morphology of NaCl Crystals: A Combined Theoretical and Simulation Study. *Fluid Phase Equilib.* **2010**, *290*, 36−42.

(17) Gee, M. B.; Cox, N. R.; Jiao, Y.; Bentinitis, N.; Weerasinghe, S.; Smith, P. E. A Kirkwood−Buff Derived Force Field for Aqueous Alkali Halides. *J. Chem. Theory Comput.* **2011**, *7*, 1369−1380.

(18) Fyta, M.; Netz, R. R. Ionic Force Field Optimization Based on Single-Ion and Ion-Pair Solvation Properties: Going beyond Standard Mixing Rules. *J. Chem. Phys.* **2012**, *136*, 124103.

(19) Lísal, M.; Smith, W. R.; Kolafa, J. Molecular Simulations of Aqueous Electrolyte Solubility: 1. The Expanded-Ensemble Osmotic Molecular Dynamics Method for the Solution Phase. *J. Phys. Chem. B* **2005**, *109*, 12956.

(20) Moučka, F.; Lísal, M.; Škvor, J.; Jirsák, J.; Nezbeda, I.; Smith, W. R. Molecular Simulation of Aqueous Electrolyte Solubility. 2. Osmotic Ensemble Monte Carlo Methodology for Free Energy and Solubility Calculations and Application to NaCl. *J. Phys. Chem. B* **2011**, *115*, 7849.

(21) Moučka, F.; Lísal, M.; Smith, W. R. Molecular Simulation of Aqueous Electrolyte Solubility. 3. Alkali-Halide Salts and Their Mixtures in Water and in Hydrochloric Acid. *J. Phys. Chem. B* **2012**, *116*, 5468.

(22) Moučka, F.; Nezbeda, I.; Smith, W. R. Molecular Force Fields for Aqueous Electrolytes: SPC/E-Compatible Charged LJ Sphere Models and Their Limitations. *J. Chem. Phys.* **2013**, *138*, 154102.

(23) Moučka, F.; Nezbeda, I.; Smith, W. R. Monte Carlo Simulations on Polarizable Models: Multi-Particle-Move Method for Water and Aqueous Electrolytes. *Mol. Simul.* **2013**, in press.

(24) Ferrario, M.; Ciccotti, G.; Cartailler, T.; Spohr, E.; Turq, P. Solubility of KF in Water by Molecular Dynamics Using the Kirkwood Integration Method. *J. Chem. Phys.* **2002**, *117*, 4947−4953.

(25) Sanz, S.; Vega, C. Solubility of KF and NaCl in Water by Molecular Simulation. *J. Chem. Phys.* **2007**, *126*, 014507.

(26) Paluch, A. S.; Jayaraman, S.; Shah, J. K.; Maginn, E. J. A Method for Computing the Solubility Limit of Solids: Application to Sodium Chloride in Water and Alcohols. *J. Chem. Phys.* **2010**, *133*, 124504.

(27) Aragones, J. L.; Sanz, E.; Vega, C. Solubility of NaCl in Water by Molecular Simulation Revisited. *J. Chem. Phys.* **2012**, *136*, 244508.

(28) Hamer, W. J.; Wu, Y.-C. Osmotic Coefficients and Mean Activity Coefficients of Univalent Electrolytes in Water at 25°C. *J. Phys. Chem. Ref. Data* **1972**, *1*, 1047−1100.

(29) Allen, M. P.; Tildesley, D. J. *Computer Simulation of Liquids*; Clarendon Press: Oxford, 1987.

(30) Frenkel, D.; Ladd, A. J. C. New Monte Carlo Method To Compute the Free Energy of Arbitrary Solids. Application to the fcc and hcp Phases of Hard Spheres. *J. Chem. Phys.* **1984**, *81*, 3188−3193.

(31) Anwar, J.; Frenkel, D.; Noro, M. G. Calculation of the Melting Point of NaCl by Molecular Simulation. *J. Chem. Phys.* **2003**, *118*, 728−735.

(32) Hummer, G.; Pratt, L. R.; Garcia, A. E. Free Energy of Ionic Hydration. *J. Phys. Chem.* **1996**, *100*, 1206−1215.

(33) Garten, V. A.; Head, R. B. Homogeneous Nucleation and the Phenomenon of Crystalloluminescence. *Philos. Mag.* **1966**, *14*, 1243−1253.

(34) Joung, I. K.; Cheatham, T. E., III. Molecular Dynamics Simulations of the Dynamic and Energetic Properties of Alkali and Halide Ions Using Water-Model-Specific Ion Parameters. *J. Phys. Chem. B* **2009**, *113*, 13279−13290.

(35) Janecek, J. Long Range Corrections in Inhomogeneous Simulations. *J. Phys. Chem. B* **2006**, *110*, 6264−6269.

(36) Rogers, P. S. Z.; Pitzer, K. S. Volumetric Properties of Aqueous Sodium Chloride Solutions. *J. Phys. Chem. Ref. Data* **1982**, *11*, 15−81.

(37) Chase, M. W., Jr. NIST-JANAF Thermochemical Tables, 4th ed. *J. Phys. and Chem. Reference Data Monograph No. 9*; American Chemical Society and American Institute of Physics: Washington, DC, 1998.

(38) Schmid, R.; Miah, A. M.; Sapunov, V. N. A New Table of the Thermodynamic Quantities of Ionic Hydration: Values and Some Applications (Enthalpy−Entropy Compensation and Born Radii). *Phys. Chem. Chem. Phys.* **2000**, *2*, 97−102.

(39) Bockris, J.; Pilla, A.; Barton, J. L. Densities of Solid Salts at Elevated Temperatures and Molar Volume Change on Fusion. *J. Phys. Chem.* **1960**, *64*, 507−508.

(40) Mancinelli, R.; Botti, A.; Bruni, F.; Ricci, M. A.; Soper, A. K. Hydration of Sodium, Potassium, and Chloride Ions in Solution and the Concept of Structure Maker/Breaker. *J. Phys. Chem. B* **2007**, *111*, 13570−13577.

(41) Joung, I. S.; Luchko, T.; Case, D. A Simple Electrolyte Solutions: Comparison of DRISM and Molecular Dynamics Results for Alkali Halide Solutions. *J. Chem. Phys.* **2013**, *138*, 044103.

(42) Shroll, M.; Smith, D. E. Molecular Dynamics Simulations in the Grand Canonical Ensemble: Formulation of a Bias Potential for Umbrella Sampling. *J. Chem. Phys.* **1999**, *110*, 8295−8302.